2018 European Control Conference (ECC)
June 12-15, 2018. Limassol, Cyprus

# Optimal Altitude Control of an Integrated Airborne Wind Energy System with Globalized Lyapunov-based Switched Extremum Seeking

Alireza Bafandeh [1] and Chris Vermillion[2]

*Abstract*— **Airborne wind energy (AWE) systems replace the tower and foundation of contemporary wind turbines with tethers and a lifting body. This enables AWE systems to adjust their operating altitudes to deliver the greatest amount of net energy possible. However, determining the optimal operating altitude requires knowledge of the wind speed vs. altitude (wind shear) profile, leading to a tradeoff between exploration and exploitation. In this work, we consider an *integrated* AWE-battery-generator system in which it is possible to explore the domain of admissible altitudes during periods of low load demand and exploit the best altitude at other times. Specifically, we propose and evaluate four candidate hierarchical structures, based on a globalized Lyapunov-based switched extremum seeking (G-LSES) control structure, for control of the integrated system. We present simulation-based results that are based on actual wind speed and load demand data.**

## I. INTRODUCTION

Typically, the average wind speed increases with altitude [1], making it desirable to install wind turbines as high as possible. However, manufacturing, construction, and installation of towers and foundations represent up to a quarter of the total cost of wind energy systems [2], and is restricting.

To address the this challenge, airborne wind energy (AWE) systems replace the tower and foundation of contemporary wind turbines with a lifting body and tether(s). Therefore, the wind turbine has access to strong wind resources at altitudes higher than existing towered wind systems can reach. Moreover, the net energy output of an AWE system can be optimized by either moving the turbine in crosswind patterns or adjusting the altitude of the system to "hunt" for the optimal wind environment.

Previous studies on enhancing AWE system power production have primarily focused on the crosswind motion. In contrast, fewer have investigated the possibility of increasing the net output energy of the system by simply optimizing the flight altitude. Within this group, used a Lyapunov-based switched extremum seeking (LSES) controller to optimize the altitude trajectory. Recognizing that LSES only achieves local optimality and does not incorporate a mechanism for considering the statistical properties of the wind shear profile, [3] proposed a model predictive control (MPC) strategy for altitude optimization. Comparing the two aforementioned controllers, LSES is local but computationally cheap, whereas MPC can be made global and can account for statistical and historical wind properties, but it is computationally expensive. In response to this observation, a fused hierarchical structure based on LSES and MPC was constructed and evaluated in [4] to leverage pros and address cons of the two techniques.

In contrast to previous work, this paper focuses on an *integrated* AWE-generator-battery system, depicted schematically in Fig. 1. For the purpose of this work, we focus on a 100kW version of the Altaeros Energies Buoyant Airborne Turbine (BAT). We propose and evaluate four candidate hierarchical control structures, each conforming to the general structure of Fig. 2, which each consist of:

1) An upper-level controller that computes (i) battery and generator setpoints, as well as (ii) an extremum seeking perturbation amplitude for altitude control, based on a confidence metric that assesses how likely it is that the AWE system is operating at its optimal altitude;
2) A middle-level LSES controller for adjusting the altitude setpoint of the AWE system;
3) A lower-level flight controller that tracks the altitude setpoint dictated by the middle level. Because lower-level flight controllers (see [5]) have already been developed and validated in the literature, our focus in this work lies in the upper and middle levels.

This fusion of an upper-level controller that determines the extremum seeking perturbation amplitude with a middle-level controller that executes LSES is termed globalized LSES (G-LSES), and was first introduced for a stand-alone AWE system (without a generator and batteries) in [6]. In this scenario, the size of the extremum seeking signal is based on a statistical measure of confidence that the AWE system is operating close to its peak power point, and the middle-level LSES algorithm itself is driven by instantaneous net power. However, in the presence of a generator and battery storage, the extremum seeking perturbation signal can instead be determined based on the confidence that the generator expenditure is being minimized (which does not always require maximum wind power output, for example when load demand is low). This study addresses the following research questions:

- What is the effect of changing the structure of objective function from maximizing net wind power output to minimizing generator power expenditure at each level of the hierarchical controller?

*This work was supported by the National Science Foundation (NSF), Award No. 1437296

[1]Alireza Bafandeh is a PhD candidate in Mechanical Engineering and Engineering Science Department, University of North Carolina at Charlotte, NC, USA abafande@uncc.edu

[2]Chris Vermillion is with faculty of Mechanical Engineering and Engineering Science Department, University of North Carolina at Charlotte, NC. He is also a Technical Advisor and equity stakeholder at Altaeros Energies, Inc., Boston, MA, USA cvermill@uncc.edu

- Based on real wind and load demand data, how do the proposed G-LSES strategies compare against legacy LSES strategies proposed in [7]?

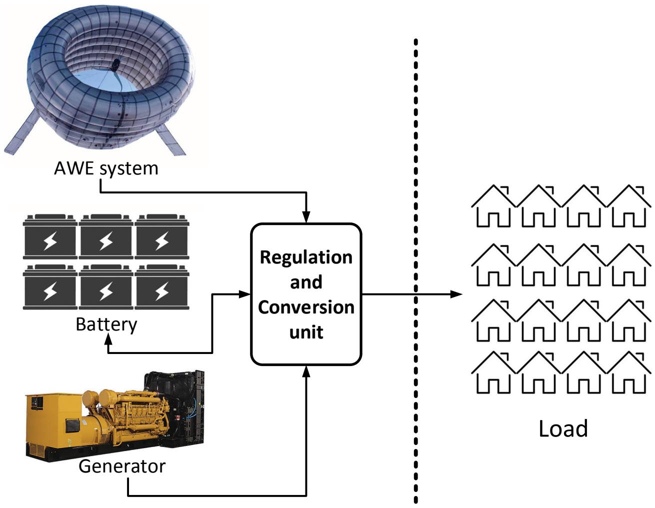


Fig. 1: Schematic of an AWE system including AWE system (here Altaeros BAT [8]), battery, and generator.

We show, through simulations based on real wind and load demand data, that the globalized control strategies outperform their local LSES counterparts. Furthermore, we show that while it is slightly beneficial to focus on generator power minimization, rather than wind power maximization, to dictate the LSES setpoint, it is extremely disadvantageous to use generator power to drive the LSES algorithm at the middle level. An explanation of why this is the case is provided in the discussion of results.

In summary, this paper makes three significant contributions relative to the existing literature:

1) We propose an AWE altitude optimization algorithm that explicitly accounts for the full integrated system (including batteries and generator);
2) Four globalized LSES (G-LSES) structures are compared against each other and against local LSES approaches proposed in previous work;
3) We present simulation-based validation of the proposed hierarchical optimization strategies for a 100kW AWE system, using real wind and load data over 28 days.

## II. WIND SHEAR PROFILE, LOAD DEMAND DATA, AND ENERGY GENERATION MODEL

### A. Wind Shear Profile and Load Demand Data

The wind data used in this study has been obtained from a radar wind profiler installed in Cape Henlopen State Park (located in Lewes, Delaware) by Dr. Christina Archer's research group at the University of Delaware [9]. The data was logged every 30 minutes at 48 different altitudes ranging from 146m to 3km. In this study, we have focused on wind data at altitudes below 1km because of regulatory limits.

Load demand data for this study were acquired from the PJM Interconnection website [10]. For the purpose of this study, hourly load data has been scaled down such that the average load demand is equal to two thirds of the rated power of the AWE system used in this research, which is a BAT system with a 100 kW wind turbine. Thus, the AWE system is sized such that it supplies a substantial fraction of the total load demand (rendering the battery storage system essential due to the high penetration of wind energy).

### B. Energy Generation Model

The net instantaneous power output of the AWE system is given by [7]:

$$P = k_1 \min(v_{\mathrm{w}}(z), v_{\mathrm{r}})^3 - k_2 v_{\mathrm{w}}^2 - \bar{k}_3 v_{\mathrm{w}}^2 |\dot{z}|, \qquad (1)$$

where $z$ is the operating altitude, $v_{\mathrm{w}}(z)$ is the wind speed at the operating altitude, $v_{\mathrm{r}}$ is the turbine's rated wind speed, and $k_1$, $k_2$, and $\bar{k}_3$ are coefficients that depend on the turbine and AWE system design. The first term in (1) represents the power output of the turbine, whereas the second and third terms account for the power required to maintain and adjust (respectively) the operating altitude of the AWE system under typical levels of turbulence.

## III. BATTERY MODEL AND GENERATOR ENERGY CALCULATION

In this study, the battery system is modeled in discrete time, using a simple difference equation. Specifically, the battery charge at time step $k+1$, denoted by $C_{\mathbf{b}}(k+1)$, is equal to the previous state of charge plus the amount of additional energy stored in or discharged from the energy storage, taking into account charging and discharging efficiency of the battery:

$$C_{\mathbf{b}}(k+1) = \begin{cases} C_{\mathbf{b}}(k) - \frac{1}{\eta_{bat}} E_{\mathbf{bat}}(k), & E_{\mathbf{bat}}(k) > 0 \\ C_{\mathbf{b}}(k) - \eta_{bat} E_{\mathbf{bat}}(k), & \text{otherwise}, \end{cases} \qquad (2)$$

where $E_{\mathbf{bat}}(k)$ is the amount of energy supplied by the battery at step $k$, and $\eta_{bat}$ is the charging/discharging efficiency.

Whenever possible, $E_{\mathbf{bat}}(k)$ is used to supply the balance of energy, termed the *deficit*, that is not provided by wind. This energy deficit, denoted by $E_{\mathbf{d}}(k)$, is given by:

$$E_{\mathbf{d}}(k) = (Q_l(k) - P_w(k))\, \Delta t \qquad (3)$$

Here, $Q_l$ and $P_w$ are load demand and AWE power output, respectively. The energy supplied by the battery, which is limited by the battery state of charge, is given by:

$$E_{\mathbf{bat}}(k) = \begin{cases} \eta_{bat} C_{\mathbf{b}}(k), & E_{\mathbf{d}}(k) > \eta_{bat} C_{\mathbf{b}}(k) \\ \frac{1}{\eta_{bat}}(C_{\mathbf{b}}(k) \\ \quad -C_{\mathbf{max}}), & E_{\mathbf{d}}(k) < \frac{1}{\eta_{bat}}(C_{\mathbf{b}}(k) - C_{\mathbf{max}}) \\ E_{\mathbf{d}}(k), & \text{otherwise} \end{cases} \qquad (4)$$

Here, $C_{\mathbf{max}}$ is the maximum capacity of the battery.

The generator is used, as a last priority, to meet the remainder of the load demand that is not supplied through either wind energy or the battery:

$$E_{\mathbf{gen}}(k) = \max\{0, E_{\mathbf{d}}(k) - E_{\mathbf{bat}}(k)\} \qquad (5)$$

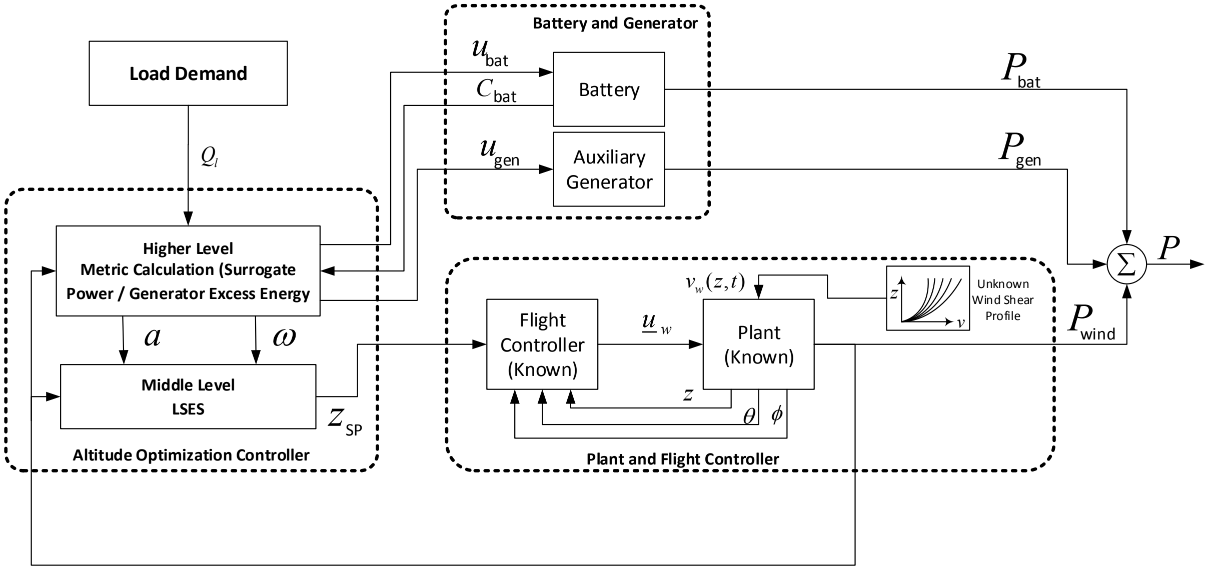


Fig. 2: Basic block diagram of G-LSES controller for altitude optimization of an integrated AWE system

## IV. ALTITUDE CONTROL VIA GLOBALIZED LYAPUNOV-BASED SWITCHED EXTREMUM SEEKING

The altitude control structure considered in this research is a variant of the Lyapunov-based switched extremum seeking detailed in [6]), where the extremum seeking perturbation size is varied based on the level of confidence that the system is operating near a global optimum. The overall structure of this controller, termed *globalized* Lyapunov-based switched extremum seeking (G-LSES), is reviewed in this section.

In the G-LSES control structure, an upper-level controller uses the conditional probability model of available wind velocity to estimate the level of confidence that the system is operating near a global optimum. This confidence is assessed using a *surrogate power deficit metric*, which is detailed in Section V. Because the upper-level controller adjusts the perturbation size, it must also adjust the perturbation frequency in order to ensure that such perturbations in altitude are achievable, given physical rate limitations on the tethers. With respect to Fig. 3, the perturbation size and frequency are denoted by $a_0$ and $\omega$, respectively. A middle-level controller executes standard LSES, which is a variant of extremum seeking where the perturbation amplitude is reduced when convergence upon a local optimum is detected. Both the upper- and middle-level controllers are detailed in the subsequent sections.

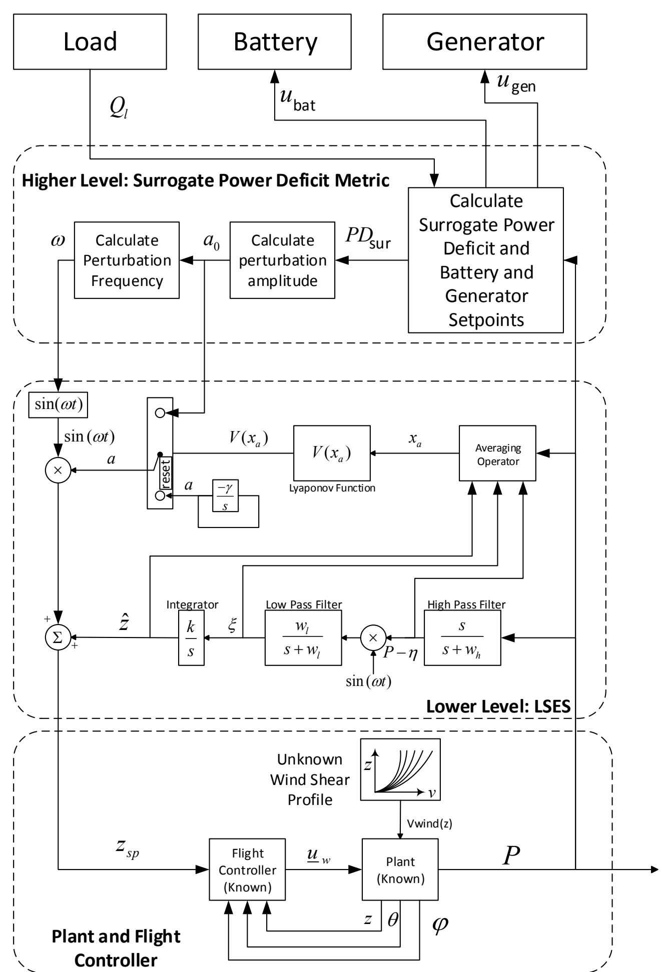


Fig. 3: G-LSES hierarchical control structure.

## V. UPPER CONTROL LEVEL - CALCULATION OF SURROGATE DEFICIT METRIC

The upper control level in the proposed hierarchical structure of Fig. 2 adapts the perturbation amplitude and frequency of the extremum seeking perturbation signal used by the middle control level, based on a statistical confidence metric. In particular, the upper-level controller seeks to answer the question: *How confident are we that the*

*AWE system is operating close to its optimal altitude?* To address this question quantitatively, we introduce in this section the *surrogate power deficit* metric, which is related to the estimated difference between the amount of power that the AWE system *could be* producing and the amount of power that it *is* producing. This power deficit can also be calculated in terms of generator power, in which case the surrogate power deficit represents an index that is related to the expected difference between the amount of power that *is presently required* by the generator and the *minimum amount of power that could be required by the generator* if the AWE were operating at its optimal altitude. Because the only available wind speed measurement is on the AWE system itself, it is impossible to quantify with certainty the difference between the power produced by the AWE system and the optimal power production value over all altitudes - hence, and estimate is required (hence the term *surrogate*). This estimate is calculated based on statistical properties of the wind, as detailed below.

### A. Statistical Wind Shear Profile Characterization

In wind energy literature, three distributions are commonly used to characterize wind velocity, including the Weibull distribution [11], Rayleigh distribution [12], and 2-parameter log normal distribution (LN2) [13]. The LN2 distribution is used by [3] and in this work to develop a conditional probability model of the wind velocity, conditioned on the previous measurements. The conditional mean and standard deviation of this model are given by:

$$\mu^c \triangleq \mu(ln(x(t,z))|\mathbf{D}) \tag{6}$$

and

$$\sigma^c \triangleq \sigma(ln(x(t,z))|\mathbf{D}), \tag{7}$$

in which the random variable $x$ is taken as the ratio of the wind velocity ($v_{wind}$) to a reference wind velocity, $v_0$:

$$x = \frac{v_{\text{wind}}}{v_0}, \tag{8}$$

and the parameters $\mu^c$ and $\sigma^c$ are the conditional mean and standard deviation of normal distribution of $ln(x)$, respectively. $\mathbf{D}$ is a matrix of $m$ previously-measured wind speeds and corresponding measurement points:

$$\mathbf{D} = \begin{bmatrix} t_0 & \dots & t_{m-1} \\ z_0 & \dots & z_{m-1} \\ v_{\text{wind}}(t_0, z_0) & \dots & v_{\text{wind}}(t_{m-1}, z_{m-1}) \end{bmatrix}. \tag{9}$$

$\mu^c$ and $\sigma^c$ are estimated as:

$$\hat{\mu}^c(ln(x(t,z))|\mathbf{D}) = \sum_{i=0}^{m-1} w_i(ln(x(t_i, z_i))), \tag{10}$$

$$\hat{\sigma}^c(ln(x(t,z))|\mathbf{D}) = m_0 \prod_{i=0}^{m-1} (1 - e^{-m_1 \Delta t_i} e^{-m_2 \Delta z_i}). \tag{11}$$

where $m_0$, $m_1$ and $m_2$ are constants and $\Delta t_i$ and $\Delta z_i$ represent the temporal and spatial differences between the present time and altitude and past measurement points.

### B. Surrogate Power Deficit Metric for Maximizing Wind Power Output

To calculate the surrogate metric, which acts as a measure of confidence in whether the AWE system is operating at a globally optimal altitude, we quantize the domain of allowable altitudes into finite number of "bins". Then, we derive a 95% confidence interval band of power output for each altitude bin. Then, we calculate the portion of this interval that exceeds the power production at the current altitude. Finally, we sum these portions over all altitude bins. The confidence interval is parameterized as follows:

$$CF_{\mathbf{lb,w}}(i) = \max\left(0, E[P](i) - 1.96 * \sigma_i\right) \tag{12}$$

$$CF_{\mathbf{ub,w}}(i) = \min\left(P_r, E[P](i) + 1.96 * \sigma_i\right) \tag{13}$$

$$\tag{14}$$

where $CF_{\mathbf{lb,w}}(i)$ and $CF_{\mathbf{ub,w}}(i)$ are the boundaries of the confidence interval of the $i^{th}$ altitude bin, $CF_i$ is the 95% confidence band, and $E[p](i)$ and $\sigma_i$ are conditional probability characteristics of the available power at altitude bin $i$.

When the objective of the upper-level controller is simply to maximize AWE power output, $PD_{\text{sur}}$ is calculated using the formula:

$$PD_{\text{sur}} = \sum_{i=1}^{n} \max(0, CF_{\mathbf{ub,w}}(i) - P_{\text{cur}}). \tag{15}$$

Here, $n$ is the number of bins, $CF_{\mathbf{ub,w}}(i)$ is the upper bound for confidence interval in the $i^{th}$ altitude bin, and $P_{\text{cur}}$ is the current power output of the system. This process is visualized in Fig. 4.

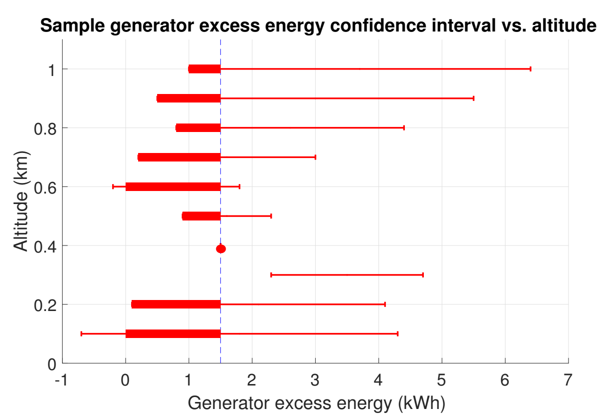


Fig. 4: Sample visualization of 95% confidence intervals for generator excess energy. Here, it is assumed the AWE system is flying at bin no. 4.

### C. *Surrogate Power Deficit Metric for Minimizing Generator Power*

In many instances when load demand is low and the battery is full, there may exist a variety of altitudes for which the AWE system meets the entire load demand. In these cases, it may not be beneficial to waste control energy searching for altitudes where the AWE power output will be greater, only to have this power output curtailed. This motivates a modified surrogate deficit metric, where we build the confidence intervals based on the generator power expenditure, $P_{\mathbf{gen}}$. Additionally, we add another term to this calculation to incentivize exploration. In order to determine this new surrogate metric, denoted by $M_{\mathbf{sur}}$, a vector of excess generator energy (i.e., the difference between the energy expended by the generator and the energy that *could be* expended by operating at the optimal altitude) for each altitude bin ($GE$) is calculated as follows:

$$GE_{\mathrm{sur}}(i) = \hat{E}_{\mathbf{gen}}(i) - \min(C_{\mathbf{max}} - C_{\mathbf{bat}}(k), P_w(k)\Delta t) \tag{16}$$

$$CF_{\mathbf{lb}}(i) = GE_{\mathrm{sur}}(i) - 1.96\sigma(i) \tag{17}$$

$$CF_{\mathbf{ub}}(i) = GE_{\mathrm{sur}} + 1.96\sigma(i) \tag{18}$$

where $\hat{E}_{\mathbf{gen}}(i)$ is the estimated generator energy corresponding to altitude bin $i$, and $CF_{\mathbf{lb}}(i)$ and $CF_{\mathbf{lb}}(i)$ are the upper and lower bounds of the surrogate metric.

The surrogate metric $M_{\mathbf{sur}}$ is sum of the portions of these confidence intervals that are less than the current energy output of the generator $E_{\mathbf{gen}}$:

$$M_{\mathbf{sur}} = \sum_{i=1}^{n} \max(0, E_{\mathbf{gen}} - CF_{\mathbf{lb}}(i)) \tag{19}$$

## VI. MIDDLE CONTROL LEVEL - LYAPUNOV-BASED SWITCHED EXTREMUM SEEKING

Extremum seeking (ES) is a real-time optimization tool to find the extremum of an unknown objective function (see [14], [15], [16]). In Conventional ES, the system can enter a limit cycle around the optimum instead of asymptotically converging to it, which leads to wasted control energy and sacrifices optimality. An ES scheme initially proposed by [17] reduces the perturbation size, $a_0$, after the system converges to a neighborhood around the optimal point. A Lyapunov function value is used to determine the required proximity to the optimum before the perturbation size is reduced. This function is based on an averaged model of the original ES feedback system. The block diagram for this Lyapunov-based switched extremum seeking (LSES) strategy is shown in Fig. 3, with reference to the AWE system (where the control variable being adjusted by extremum seeking is the altitude setpoint, $z_{sp}$).

Here, we use the same LSES scheme as detailed in [18].

TABLE I: AWE System Parameters

| Parameter | Description | Value |
|---|---|---|
| total time | individual simulation period | 28 days |
| $v_{\mathrm{r}}$ | Turbine rated wind speed | 12 m/s |
| $z_h$ | Max. allowable altitude | 1.04 km |
| $z_l$ | Min. allowable altitude | 0.146 km |
| $r_z$ | Rate of altitude change | 0.3 m/s |
| $k_1$ | Coefficient in 1 | 0.0579 $\frac{kWs^3}{m^3}$ |
| $k_2$ | Coefficient in 1 | 0.09 $\frac{kWs^2}{m^2}$ |
| $k_3$ | Coefficient in 1 | 1.08 $\frac{kWs^3}{m^3}$ |

TABLE II: LSES Parameters

| Parameter | Description | Value |
|---|---|---|
| $k_{\mathrm{wind}}$ | Integrator Gain when the objective is to maximize the net power | $3e-5$ kW/m |
| $k_{\mathrm{gen}}$ | Integrator Gain when the objective is to minimize the generator power | $-5e-7$ kW/m |
| $a$ | Perturbation magnitude | 10 m |
| $a_{\mathrm{min}}$ | Minimum perturbation magnitude | 5 m |
| $\omega$ | Perturbation frequency | 1.5708 rad/min |
| $\omega_H$ | High-pass filter frequency | 1.4137 rad/min |
| $\omega_L$ | Low-pass filter frequency | 0.1414 rad/min |
| $\epsilon$ | Switching threshold | $1e-9$ |

## VII. RESULTS

The AWE system with a G-LSES hierarchical control structure has been simulated for different combinations of objective functions at the two control levels, using real wind velocity and load demand data obtained from [9] and PJM, respectively. The simulations have been performed over a period of 28 days. Tables I and II give the values of the parameters used in simulations.

Six different control scenarios have been considered in our simulations, two of which represent stand-alone LSES strategies (where the extremum seeking perturbation size cannot be enlarged by an upper-level controller) and four of which represent G-LSES strategies:

*a) Scenario 1: LSES Standalone with Wind Power (LSES with Wind):* This controller is a single level LSES (with no upper-level controller to adjust the extremum seeking perturbation size), where the objective function (to be maximized) is equal to the instantaneous power output of the AWE system.

*b) Scenario 2: LSES Standalone with Generator Setpoint (LSES with Gen):* This controller is a single level LSES (with no upper-level controller to adjust the extremum seeking perturbation size), where the objective function (to

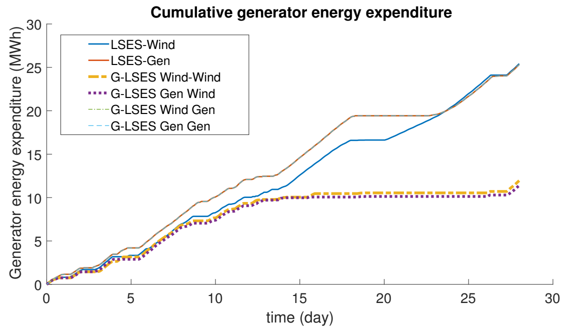


Fig. 5: Generator power set-point for 6 control scenarios.

be minimized) is the instantaneous generator power set-point of the AWE system.

*c) Scenario 3: Globalized LSES with Wind Power at Both Levels (Wind - Wind):* This controller is a hierarchical G-LSES controller wherein the objective function at both levels is the instantaneous wind power output of the system.

*d) Scenario 4: Globalized LSES with Generator Set-point at Upper and Wind Power at Lower Control Level (Gen - Wind):* This is a hierarchical G-LSES controller where the objective function at the upper level is the instantaneous generator power (to be minimized), whereas the lower level objective function is the instantaneous wind power output (to be maximized).

*e) Scenario 5: Globalized LSES with Wind Power at Upper and Generator Set-point at Lower Control Level (Wind - Gen):* This is a hierarchical G-LSES controller where the objective function at the upper level is the instantaneous power output of the AWE system, whereas the lower level objective function is the instantaneous generator power.

*f) Scenario 6: Globalized LSES with Generator Set-point at Both Levels (Gen - Gen):* This is a hierarchical G-LSES controller where the objective function at both levels is the instantaneous generator power (to be minimized).

Fig. 5 compares the excess energy that is required to be supplied from the auxiliary generator for each control scenario, based on the simulations for 28 days using actual wind velocity and load demand data. This figure shows that considering generator power at the upper level and raw wind power at the middle level (Gen - Wind scenario) results in the highest renewable energy penetration, followed by the strategy of basing both the upper and middle level controllers on wind power.

## VIII. CONCLUSION AND FUTURE WORK

In this paper, we have shown through simulation, using real wind and load demand data, that globalized Lyapunov-based switched extremum seeking (G-LSES) can improve performance of an integrated AWE system when compared with stand-alone LSES. Furthermore, we compared various implementations of G-LSES. We concluded that while it is slightly beneficial to consider generator energy expenditure, rather than wind power production, when determining the extremum seeking perturbation size, it is essential to use wind power production to drive the LSES algorithm itself. Future work will investigate means by which formal global convergence properties can be guaranteed, under reasonable limiting assumptions, for the G-LSES strategies proposed in this work.

## REFERENCES


[1] J. F. Manwell, J. G. McGowan, and A. L. Rogers, *Wind energy explained: theory, design and application*. John Wiley and Sons, 2010.

[2] "Renewable energy technologies: Cost analysis series," International Renewable Energy Agency, Report, 2012.

[3] S. Bin-Karim, A. Bafandeh, and C. Vermillion, "Spatio-temporal optimization through model predictive control: A case study in airborne wind energy," in *2016 IEEE 55th Conference on Decision and Control (CDC)*, Conference Proceedings.

[4] A. Bafandeh, S. Bin-Karim, and C. Vermillion, "Fused local-global control of spatiotemporally-varying systems, a case study in airborne wind energy," in *IEEE Conference on Control Technology and Applications (CCTA), 2017*. Kohala Coast, Hawaii: IEEE, Conference Proceedings.

[5] C. Vermillion, T. Grunnagle, and I. Kolmanovsky, "Modeling and control design for a prototype lighter-than-air wind energy system," in *American Control Conference (ACC)*. Montreal, QC, Canada: IEEE, 2012, Conference Proceedings, pp. 5813–5818.

[6] A. Bafandeh, S. Bin-Karim, A. Baheri, and C. Vermillion, "Altitude optimization of airborne wind energy systems via switched extremum seeking–design, analysis, and economic assessment," *Control Engineering Pratice (accepted awaiting publishing)*.

[7] A. Bafandeh and C. Vermillion, "Altitude optimization of airborne wind energy systems via switched extremum seeking–design, analysis, and economic assessment," *IEEE Transactions on Control Systems Technology*, vol. PP, no. 99, pp. 1–12, 2017.

[8] "Altaeros Energies Website http://www.altaerosenergies.com/."

[9] C. Archer, "Wind profiler at cape henlopen, lewes, delaware , http://www.ceoe.udel.edu/our-people/profiles/carcher/fsmw," University of Delaware, Report.

[10] "Estimated hourly load for pjm region," 2016. [Online]. Available: http://www.pjm.com/markets-and-operations/energy/real-time/loadhryr.aspx

[11] J. E. Pinder, J. G. Wiener, and M. H. Smith, "The weibull distribution: a new method of summarizing survivorship data," *Ecology*, vol. 59, no. 1, pp. 175–179, 1978.

[12] D. Kundu and M. Z. Raqab, "Generalized rayleigh distribution, different methods of estimations," *Computational statistics and data analysis*, vol. 49, no. 1, pp. 187–200, 2005.

[13] S. Mandal and M. J. Ali, "Log-normal distribution," 2015.

[14] K. B. Ariyur and M. Krstic, *Real-time optimization by extremum-seeking control*. John Wiley and Sons, 2003.

[15] H.-H. Wang and M. Krstic, "Extremum seeking for limit cycle minimization," *Automatic Control, IEEE Transactions on*, vol. 45, no. 12, pp. 2432–2436, 2000.

[16] M. Krstić and H.-H. Wang, "Stability of extremum seeking feedback for general nonlinear dynamic systems," *Automatica*, vol. 36, no. 4, pp. 595–601, 2000.

[17] S. J. Moura and Y. A. Chang, "Asymptotic convergence through lyapunov-based switching in extremum seeking with application to photovoltaic systems," in *American Control Conference (ACC)*. Baltimore, MD: IEEE, 2010, Conference Proceedings.

[18] A. Bafandeh and C. Vermillion, "Real-time altitude optimization of airborne wind energy systems using lyapunov-based switched extremum seeking control," in *American Control Conference (ACC), 2016*. Boston, MA: IEEE, Conference Proceedings.